Cerebral Cortex, 2022;32: 1295–1306

https://doi.org/10.1093/cercor/bhab294
Advance Access Publication Date: 27 August 2021
Original Article

ORIGINAL ARTICLE

Human Cerebral Perfusion, Oxygen Consumption, and Lactate Production in Response to Hypoxic Exposure

Mark B. Vestergaard[1], Hashmat Ghanizada[2], Ulrich Lindberg[1], Nanna Arngrim[2], Olaf B. Paulson[3,4], Albert Gjedde[5,6], Messoud Ashina[2,4] and Henrik B.W. Larsson[1,4]

[1]Functional Imaging Unit, Department of Clinical Physiology, Nuclear Medicine, and PET, Copenhagen University Hospital Rigshospitalet, Glostrup 2600, Denmark, [2]Danish Headache Center, Department of Neurology, Copenhagen University Hospital Rigshospitalet, Glostrup 2600, Denmark, [3]Neurobiology Research Unit, Department of Neurology, Copenhagen University Hospital Rigshospitalet, Copenhagen 2100, Denmark, [4]Faculty of Health and Medical Science, Department of Clinical Medicine, University of Copenhagen, Copenhagen 2100, Denmark, [5]Faculty of Health and Medical Science, Department of Neuroscience, University of Copenhagen, Copenhagen 2100, Denmark and [6]Translational Neuropsychiatry Unit, Department of Clinical Medicine, Aarhus University, Aarhus 8000, Denmark

Address correspondence to Henrik B.W. Larsson, Department of Clinical Physiology, Nuclear Medicine and PET, Rigshospitalet, Valdemar Hansens Vej 1-23, Glostrup 2600, Denmark. Email: henrik.bo.wiberg.larsson@regionh.dk

Abstract

Exposure to moderate hypoxia in humans leads to cerebral lactate production, which occurs even when the cerebral metabolic rate of oxygen ($CMRO_2$) is unaffected. We searched for the mechanism of this lactate production by testing the hypothesis of upregulation of cerebral glycolysis mediated by hypoxic sensing. Describing the pathways counteracting brain hypoxia could help us understand brain diseases associated with hypoxia. A total of 65 subjects participated in this study: 30 subjects were exposed to poikilocapnic hypoxia, 14 were exposed to isocapnic hypoxia, and 21 were exposed to carbon monoxide (CO). Using this setup, we examined whether lactate production reacts to an overall reduction in arterial oxygen concentration or solely to reduced arterial oxygen partial pressure. We measured cerebral blood flow (CBF), $CMRO_2$, and lactate concentrations by magnetic resonance imaging and spectroscopy. CBF increased ($P < 10^{-4}$), whereas the $CMRO_2$ remained unaffected ($P > 0.076$) in all groups, as expected. Lactate increased in groups inhaling hypoxic air (poikilocapnic hypoxia: 0.0136 $\frac{\text{mmol/L}}{\Delta S_aO_2}$, $P < 10^{-6}$; isocapnic hypoxia: 0.0142 $\frac{\text{mmol/L}}{\Delta S_aO_2}$, $P = 0.003$) but was unaffected by CO ($P = 0.36$). Lactate production was not associated with reduced $CMRO_2$. These results point toward a mechanism of lactate production by upregulation of glycolysis mediated by sensing a reduced arterial oxygen pressure. The released lactate may act as a signaling molecule engaged in vasodilation.

Key words: cerebral blood flow, cerebral hemodynamics, cerebral metabolism, hypoxia, lactate

Introduction

Acute brain hypoxia causes a decline in cognitive function in mild cases, but in severe cases leads to neuronal dysfunction, unconsciousness, and cell death. Short intermittent episodes of moderate hypoxia cause cell apoptosis, which over time leads to substantial brain atrophy (Greijer and Van Der Wall 2004; Xu et al. 2004; Sendoel and Hengartner 2014) and may be part of the pathophysiology of neurodegenerative diseases, most notably Alzheimer's disease (Zhang and Le 2010). Protection against brain hypoxia and ensuring oxygen and metabolic substrate

availability is therefore vital to the maintenance of a healthy brain.

A major protective mechanism active against brain hypoxia is the cerebrovascular reactivity (CVR), which increases cerebral blood flow (CBF) and thereby the oxygen supply to the brain. In addition, detection of a reduced oxygen pressure in cells initiates multiple compensatory mechanisms mediated by the transcription factor hypoxia-inducible factor (HIF), which upregulates gene expression related to glycolysis, glucose transport across membranes, and vascularization (Semenza 2012; Prabhakar and Semenza 2015).

Exposure to moderate poikilocapnic hypoxic air, in addition to an increase in CBF, robustly promotes cerebral lactate production in the human brain (Overgaard et al. 2012; Vafaee et al. 2012; Harris et al. 2013; Vestergaard et al. 2016, 2020). Lactate production is also observed when the cerebral metabolic rate of oxygen ($CMRO_2$) is maintained and, therefore, is likely not to arise from insufficient oxidative metabolism. Here, the increase did not follow increased systemic blood lactate levels, as the subjects remained immobile during the exposure (Vestergaard et al. 2016; Jensen et al. 2018).

We hypothesized that the upregulation of glycolysis and consequent lactate production in healthy humans is a protective mechanism activated by sensing hypoxia. The discovery of molecules and pathways involved in the activation of these defensive mechanisms will help achieve a better understanding of the protective mechanism, potentially leading to the identification of therapeutic targets against adverse brain hypoxia.

We examined three groups of human volunteers inhaling hypoxic air with freely fluctuating blood CO_2 pressure (poikilocapnic hypoxia), hypoxic air with added CO_2 (isocapnic hypoxia), or atmospheric air after saturating part of the blood with carbon monoxide (CO). The addition of CO_2 to hypoxic air eliminates the tissue alkalosis induced by hyperventilation, leading to a state of isocapnic hypoxia. Exposure to CO causes CO molecules to bind to hemoglobin, effectively lowering the oxygen concentration of the arterial blood (C_aO_2). However, exposure to CO does not lead to hyperventilation and hypocapnia or affect the arterial oxygen partial pressure (P_aO_2), in contrast to inhalation of hypoxic air (Paulson et al. 1973; Ghanizada et al. 2018). By examining these three groups, we distinguished between lactate production from overall reduced C_aO_2, which will be present in all groups, and lactate production only in the presence of a reduced P_aO_2. In addition, by comparing the results of the groups exposed to poikilocapnic and isocapnic hypoxia, we established whether tissue alkalosis was involved in lactate production. High pH levels are known to stimulate the key glycolytic enzyme phosphofructokinase (PFK), resulting in upregulation of glycolysis and increased lactate production (Trivedi and Danforth 1966).

We reasoned that if we observed lactate production in the presence of a maintained $CMRO_2$, the cause of elevated lactate would not be impaired oxidative metabolism or tissue alkalosis. Rather, elevated lactate production is more likely the result of an upregulation of glycolysis mediated by the effects of hypoxia. The upregulation of glycolysis with lactate as the end-product could then be part of a mechanism protecting against brain hypoxia.

To test the hypothesis in these three groups, we acquired measurements of CBF and $CMRO_2$ with phase-contrast magnetic resonance imaging (MRI) techniques and measurements of cerebral lactate, N-acetylaspartate (NAA), and combined creatine and phosphocreatine (Cr + PCr) concentrations with magnetic resonance spectroscopy (MRS).

Materials and Methods

In total, 65 subjects were enrolled in this study. In the group exposed to poikilocapnic hypoxia, 30 subjects participated (11 women, mean age = 26.8 years, range = 20.0–39.7 years); in the group exposed to isocapnic hypoxia, 14 subjects participated (three women, mean age = 24.4 years, range = 20.6–33.0 years); and in the group exposed to CO, 21 subjects participated (11 women, mean age = 23.1 years, range = 18.7–30.2 years). The participants had no known heart, lung, or neurological diseases. This study was approved by the Capital Region of Denmark's Committee on Health Research Ethics (H-15003589 and H-17016387) and was conducted according to the Declaration of Helsinki. All subjects gave written informed consent before participation. Data from a subset of the group inhaling hypoxic air have previously been published as control data in a study examining the cerebrovascular physiology of experienced freedivers (Vestergaard and Larsson 2019) and as part of a study on the effect of healthy aging on cerebral physiology (Vestergaard et al. 2020). An analysis and exploration of the development of headache in the group exposed to CO enrolled in the present study will be published elsewhere.

Experimental Design

All MRI scans were performed on a Philips 3 T dSTREAM Achieva MRI scanner (Philips Medical Systems) using a 32-channel phased array head coil. The experiment consisted of one MRI session including anatomical scans and the acquisition of global CBF using phase-contrast mapping (PCM), global $CMRO_2$ using susceptibility-based oximetry (SBO) (Jain et al. 2010), and cerebral lactate concentration using MRS. Global CBF, $CMRO_2$, and lactate were initially acquired during normoxia, and the acquisitions were repeated during the inhalation of hypoxic air or after the inhalation of CO. All measurements were performed in the hypoxia studies. In the CO inhalation studies, CBF was measured in all subjects, but $CMRO_2$ and lactate concentrations were measured in only a subset of 14 of the 21 subjects. The timing of the acquisitions of the MRI sequences is shown in Figure 1.

During normoxia measurements, the subjects inhaled atmospheric air from the surrounding environment. In the two groups inhaling hypoxic air (10–14% fractional oxygen), the subjects were fitted with a face mask covering the mouth and nose while lying in the scanner. The mask was connected by a tube and a one-way valve to an AltiTrainer system (SMTEC) that provided hypoxic air. A one-way valve in the mask ensured that no rebreathing was possible. End-tidal O_2 pressure ($P_{et}O_2$) and end-tidal CO_2 pressure ($P_{et}CO_2$) were measured from a tube connected to the mask by a Veris Monitor system (MEDRAD). Heart rate and arterial oxygen saturation were measured continuously throughout the scan by fingertip pulse oximetry, also using the Veris Monitor. Before the scan, a venous blood sample was drawn and analyzed immediately for hemoglobin and hematocrit using a Radiometer ABL800 Flex (Radiometer).

In the group exposed to isocapnic hypoxia, CO_2 was added to the inhaled hypoxic air to maintain a normal end-tidal CO_2 pressure. CO_2 was gradually added to each subject's air to maintain individual CO_2 levels. On average, 1.3 kPa CO_2 was added to the inhaled air (Fig. 1B).

The group exposed to CO was first scanned during normoxia. The subjects were then taken from the scanner and brought to an adjacent room where they were fitted with a full-face mask

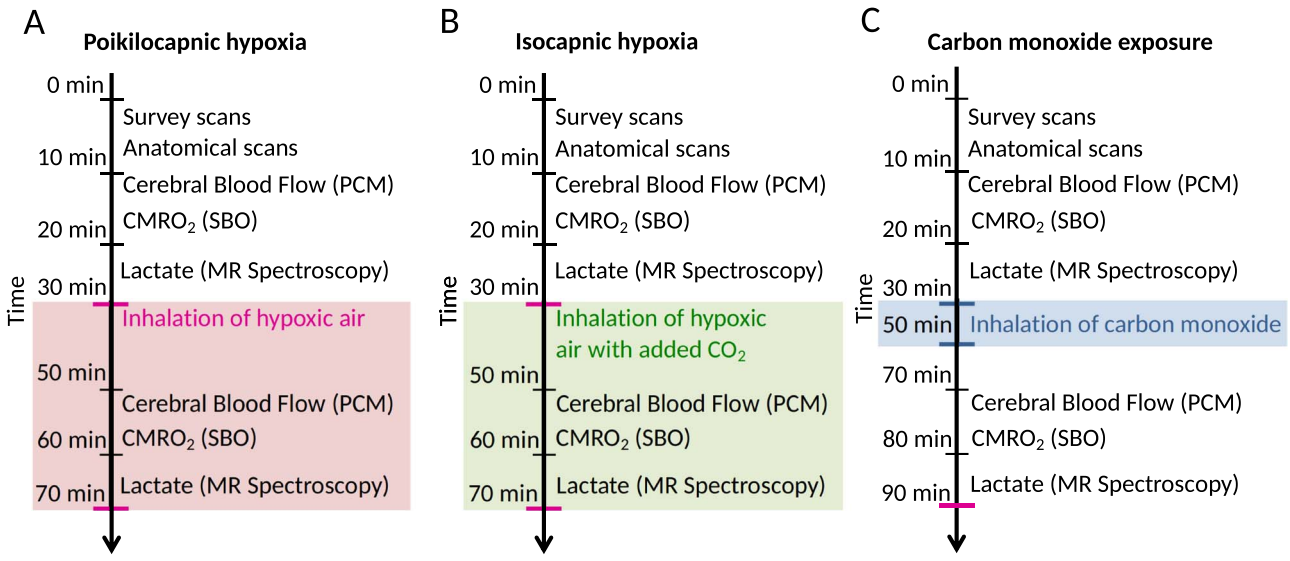

Figure 1. Timing of the acquired MRI sequences. In total, 65 subjects participated in the study. A total of 30 subjects were included in the group exposed to poikilocapnic hypoxia (*A*), 14 subjects were included in the group exposed to isocapnic hypoxia (*B*), and 21 subjects were included in the group exposed to CO (*C*). Initially, surveys and anatomical scans were obtained. Hereafter, global CBF, combined oxygen saturation and blood flow in the sagittal sinus for the calculation of $CMRO_2$, and MR spectroscopy for lactate concentration were acquired at baseline and during inhalation of hypoxic air or after exposure to carbon monoxide.

connected to a tube through which CO was provided from a gas bottle (99.997% purity, Strandmoellen). The subjects were instructed to take deep breaths and exhale slowly while CO was added to the tube. In total, each participant inhaled air with added CO three times. At baseline and after an initial inhalation of 200 mL CO, a capillary blood sample was taken and analyzed on site to determine the carboxyhemoglobin concentration (COHb). The volume of CO necessary to increase the COHb to ~22% was then calculated and given as a second and third inhalation with a regular COHb measurement in between. A mean volume of 363 ± 64 mL of CO was administered, and the participants reached a mean COHb of 21.9 ± 1.2%.

MRI Sequences

Structural Imaging

Structural images were acquired using a 3D T_1-weighted turbo field echo sequence [field of view (FOV) = 241 × 180 × 165 mm^3; voxel size = 1.1 × 1.1 × 1.1 mm^3; echo time (TE) = 2.78 ms; repetition time (TR) = 6.9 ms; flip angle = 9°]. The structural images were segmented for gray matter, white matter, and cerebrospinal fluid (CSF) using the FSL-functions BET and FAST (FMRIB Software Library, Oxford University) (Jenkinson et al. 2012). A whole-brain mask covering the cerebrum, cerebellum, and brainstem was created to obtain the total brain volume. An example of brain segmentation is shown in Figure 2E.

Cerebral Blood Flow

The mean global CBF was obtained using velocity-sensitive PCM MRI (Bakker et al. 1996; Vestergaard et al. 2017). Blood velocity contrast maps were acquired with a turbo field echo sequence (one slice, FOV = 240 × 240 mm^2; voxel size = 0.75 × 0.75 × 8 mm^3; TE = 7.33 ms; TR = 27.63 ms; flip angle = 10°; velocity encoding = 100 cm/s, without cardiac gating). Two measurements were obtained: one with the imaging plane perpendicular to the carotid arteries and one perpendicular to the basilar artery. An example of the planning and an acquired velocity-encoding map can be seen in Figure 2A and B.

The blood flows in each of the cerebral feeding arteries (both internal carotids and the basilar artery) were calculated by multiplying the mean blood velocity by the cross-sectional area from regions of interest (ROIs) defining each vessel. The global mean CBF was calculated by normalizing the total blood flow from each artery to the total brain weight. Brain weight was estimated from the segmentation of the structural MRI images assuming a brain density of 1.05 g/mL (Torack et al. 1976).

The cerebral delivery of oxygen (CDO_2) was calculated by multiplying CBF by the arterial oxygen concentration, calculated as arterial oxyhemoglobin saturation (S_aO_2) multiplied by hemoglobin concentration.

Cerebral Metabolic Rate of Oxygen

The mean global $CMRO_2$ was obtained by acquiring the flow (BF_{ss}) and venous oxyhemoglobin saturation (S_vO_2) of the blood leaving the brain in the sagittal sinus using the Fick principle:

$$CMRO_2 = [Hgb] \bullet (BF_{ss}) \bullet (S_aO_2 - S_vO_2) \quad (1)$$

The hemoglobin concentration (Hgb) is the oxygen-carrying concentration (in mmol/L) measured from venous blood samples drawn immediately before the MRI scan. The blood flow and oxygen saturation in the sagittal sinus were acquired using a dual-echo gradient-echo sequence (one slice, FOV = 220 × 190 mm^2; voxel size = 0.5 × 0.5 × 8 mm^3; TE_1 = 10.89 ms; TE_2 = 24.16 ms; flip angle = 30°; five repeated measures, velocity encoding = 100 cm/s, total duration = 1 min 30 s; SENSE-factor = 2) and combining PCM and SBO techniques. The imaging plane was located perpendicular to the sagittal sinus. BF_{ss} was calculated similarly to the processing of global CBF values described earlier by calculating a velocity-encoded image and drawing an ROI covering the vessel. The acquired blood flow in the sagittal sinus was scaled to the ratio between the global CBF and BF_{ss} measured at baseline in each participant to normalize the $CMRO_2$ to the individual global brain values. The oxygen saturation was calculated using SBO techniques, which

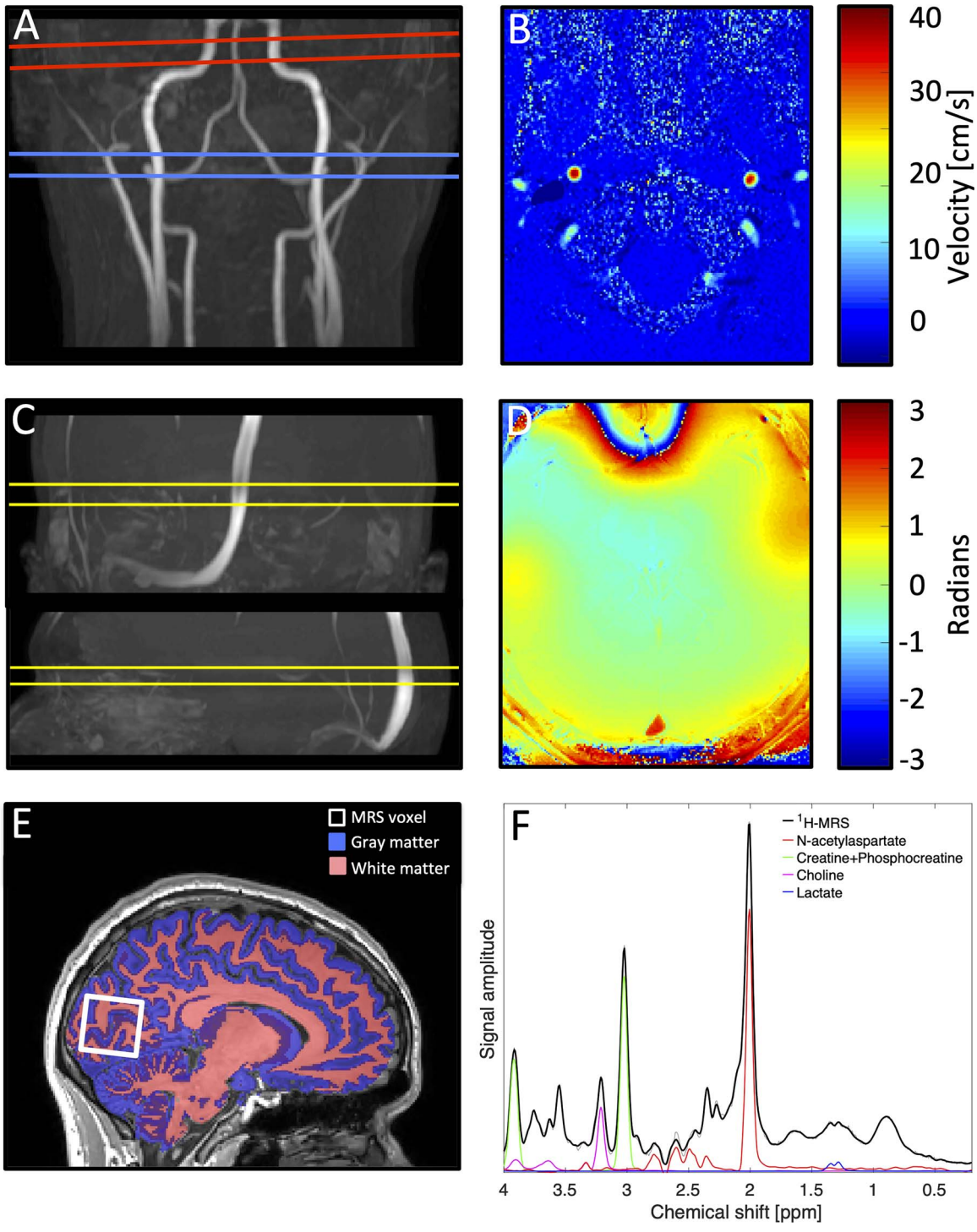

Figure 2. Examples of the magnetic resonance imaging and spectroscopy techniques used in the present study. (*A*) Demonstration of the imaging planes perpendicular to the carotid arteries (blue lines) and the basilar artery (red lines) for acquiring blood flow by velocity-encoding phase-contrast mapping. (*B*) Demonstration of an acquired velocity map with the blood velocity in the carotid arteries clearly visible. (*C*) Demonstration of the imaging plane perpendicular to the sagittal sinus in the coronal and sagittal projection for obtaining the blood flow and oxygen saturation by sequence combining phase-contrast mapping and susceptibility-based oximetry. (*D*) Susceptibility-based maps demonstrating the difference in phase values from the short and long echo times. The difference in the magnetic susceptibility of the desaturated blood in the sagittal sinus and the surrounding tissue is clearly visible. (*E*) Sagittal view of the high-resolution anatomical scan with the segmentation of gray and white matter. The location of the MR spectroscopy voxel used in the study is visualized. (*F*) Example of an acquired spectrum after postprocessing using LCModel.

utilize the fact that the difference in magnetic susceptibility between deoxyhemoglobin in venous blood and the surrounding tissue can be related to oxygen saturation (Jain et al. 2010, 2011). Susceptibility-weighted maps were calculated as the differences in phase-value maps between the first and second echoes. Aliased phase values in the sagittal sinus and the immediately surrounding tissue were manually corrected. An in-depth discussion of the sequence and postprocessing has been reported previously (Rodgers et al. 2016; Vestergaard and Larsson 2019). The method has been validated using blood sampling from the jugular vein (Miao et al. 2019). An example of the planning and an acquired susceptibility-weighted map is presented in Figure 2C and D.

MR Spectroscopy

Lactate, Cr + PCr, and NAA concentrations were obtained by MRS using a water-suppressed point-resolved spectroscopy pulse sequence (TR = 3000 ms; TE = 36 ms; voxel size = 30 × 35 × 30 mm^3). The MRS voxel was placed in the occipital lobe. Postprocessing and quantification of the metabolite concentrations were performed using LCModel (LCModel, Version 6.3-1F). The concentrations of lactate, Cr + PCr, and NAA were quantified by comparing the area under the curve of each metabolite peak in the spectrum to the area under the curve of the measured water peak (Christiansen et al. 1993). The concentration of water was estimated from the ratio of gray matter, white matter, and CSF in the MRS voxel acquired from the segmentation of the anatomical images, and assuming water concentrations of 43.3, 35.88, and 55.556 M in gray matter, white matter, and CSF, respectively (Quadrelli et al. 2016). An investigator blinded to the group assignments excluded spectra of poor quality wherein the quantification of lactate was erroneous.

An example of the location of the MRS voxel, the segmentation of gray and white matter, and an acquired spectrum is shown in Figure 2E and F.

Statistical Analysis

The postprocessing of the data was blinded to the subject's group assignment and measurement (baseline measurement or gas challenge measurement). Values are presented as the mean ± standard deviation. *P*-values <0.05 were considered significant.

The differences in the average values of the measured parameters between baseline and during exposure to hypoxia were tested by paired Student's *t*-tests (Table 1). The effects on the measurements of CBF, CDO_2, $CMRO_2$, NAA, Cr + PCr, and lactate concentration from the gas challenge (poikilocapnic hypoxia, isocapnic hypoxia, or CO exposure) were additionally assessed by a linear mixed model with the acquired parameter as the response variable (Y), arterial oxyhemoglobin saturation (S_aO_2) as the fixed effect, and subject as the random effect (u). To test whether the responses were different for the three groups, a categorical fixed effect (G) indicating group (poikilocapnic hypoxia, isocapnic hypoxia, or CO exposure) and the interaction between S_aO_2 and group indication were added to the model (eq. 2). The significance of the interaction term (β_3) indicates whether poikilocapnic hypoxia, isocapnic hypoxia, or CO state had different effects on the acquired parameters with regard to oxygen desaturation (Gujarati 1970).

$$Y_t = \beta_0 + \beta_1 \cdot S_aO_2 + \beta_2 \cdot G + \beta_3 \cdot S_aO_2 \cdot G + u \quad (2)$$

Table 1 Mean values of the acquired parameters at baseline and following poikilocapnic hypoxia (10–14% fractional oxygen in inhaled air), isocapnic hypoxia (10–14% fractional oxygen and ~1% CO_2 in inhaled air), and CO inhalation (~22% hemoglobin bound as COHb)

	Poikilocapnic hypoxia				Isocapnic hypoxia				CO exposure			
Parameters	Baseline	Hypoxia	% Change	*P*-value	Baseline	Hypoxia	% Change	*P*-value	Baseline	CO	% Change	*P*-value
S_aO_2 [%]	97.2 ± 1.1	76.1 ± 7.2	−21.8	$<10^{-6}$*	97.9 ± 1.72	82.5 ± 3.6	−15.8	$<10^{-6}$*	98.0	79.4 ± 1.6	−19.0	$<10^{-6}$*
S_vO_2 [%]	68.9 ± 7.8	55.1 ± 8.5	−19.5	$<10^{-6}$*	69.3 ± 5.3	57.2 ± 4.9	−17.4	$<10^{-5}$*	69.7 ± 7.8	56.1 ± 8.4	−19.5	$<10^{-6}$*
$P_{et}CO_2$ [kPa]	4.9 ± 0.5	3.7 ± 0.7	−25.8	$<10^{-6}$*	4.8 ± 0.3	4.8 ± 0.3	−1.2	0.37				
$P_{et}O_2$ [kPa]	12.0 ± 1.9	6.3 ± 1.8	−47.6	$<10^{-6}$*	13.2 ± 3.2	6.7 ± 1.0	−49.4	$<10^{-6}$*				
CBF [mL/100 g/min]	51.3 ± 5.5	60.7 ± 9.9	19.3	$<10^{-4}$*	61.9 ± 8.8	70.9 ± 11.1	14.9	$<10^{-3}$*	57.3 ± 7.9	75.9 ± 9.7	33.0	$<10^{-6}$*
CDO_2 [μmol/100 g/min]	457.4 ± 59.2	406.6 ± 56.0	−10.5	$<10^{-4}$*	551.0 ± 78.9	534.0 ± 80.5	−2.8	0.22	489.8 ± 58.8	525.8 ± 55.3	7.8	$<10^{-3}$*
$CMRO_2$ [μmol/100 g/min]	140.1 ± 30.0	149.8 ± 42.9	7.6	0.16	156.8 ± 22.7	163.4 ± 27.0	4.8	0.31	146.6 ± 44.8	158.6 ± 60.3	6.9	0.12
Lactate [mmol/L]	0.54 ± 0.24	0.82 ± 0.30	71.0	$<10^{-6}$*	0.48 ± 0.16	0.68 ± 0.28	48.7	0.018*	0.56 ± 0.18	0.59 ± 0.22	9.5	0.48
NAA [mmol/L]	9.3 ± 0.6	9.2 ± 0.7	−1.0	0.35	9.3 ± 0.4	9.6 ± 0.6	2.9	0.25	9.2 ± 0.5	9.2 ± 0.8	0.1	0.97
Cr + PCr [mmol/L]	6.4 ± 0.6	6.4 ± 0.6	0.4	0.92	6.6 ± 0.5	6.7 ± 0.4	2.3	0.52	6.6 ± 0.6	6.4 ± 0.7	−2.2	0.17

* denotes statistical significance

Results

One subject in the group inhaling hypoxic air and one subject in the group exposed to CO had inaccurate lactate measurements due to excessive signal from lipids originating from the scalp and soft tissue outside the brain contaminating the lactate peak. These two measurements were excluded from the analysis. Two volunteers in the isocapnic group had unacceptably wide peaks in the spectrum during inhalation of hypoxic air due to inaccurate shimming of the magnetic field for MRS acquisition. MRS data from these measurements were excluded from further analysis. Two subjects inhaling hypoxic air had bifurcations of the sagittal sinus, making the measurement of oxygen saturation unreliable, as bifurcations introduce inaccuracies into the technique (Li et al. 2012). These two measurements were excluded from further analysis.

S_aO_2, $P_{et}O_2$, $P_{et}CO_2$, and heart rate during the inhalation of hypoxic air and arterial oxyhemoglobin saturation after exposure to CO are shown in Figure 3. The correlations between oxyhemoglobin saturation and the cerebral physiology measures for the three groups are shown in Figure 4. The mean values are presented in Table 1.

"S_aO_2" declined in the poikilocapnic hypoxia group to $76.1 \pm 7.2\%$, and in the isocapnic group, it declined to $82.5 \pm 3.6\%$ at the time of MRS acquisition. After exposure to CO, the oxyhemoglobin saturation decreased to $79.4 \pm 1.9\%$ at the time of the acquisition of the MRI parameters.

"$P_{et}CO_2$" decreased from 4.9 ± 0.5 kPa in normoxia to 3.7 ± 0.7 kPa in the poikilocapnic hypoxia group and was unchanged in the isocapnic hypoxia group at the time of the acquisition of MRI parameters.

"CBF" increased in all groups (Fig. 4A). CO induced a significantly higher CBF response than hypoxic air (poikilocapnic hypoxia: $P < 10^{-6}$, isocapnic hypoxia: $P < 10^{-3}$).

"CDO_2" decreased in the poikilocapnic hypoxia group ($P < 10^{-3}$), was unchanged in the isocapnic hypoxia group ($P = 0.15$), and increased in the group exposed to CO ($P < 10^{-3}$) (Fig. 4B). The higher CDO_2 response in the CO group was significantly different from those of the hypoxic air groups (poikilocapnic hypoxia: $P < 10^{-5}$, isocapnic hypoxia: $P < 10^{-3}$).

"$CMRO_2$" was unaffected in all groups (Fig. 4C).

The "cerebral lactate" increased significantly in the poikilocapnic group ($\beta = 0.0136 \frac{\text{mmol/L}}{\Delta S_aO_2}$, $P < 10^{-6}$) and in the isocapnic hypoxia group ($\beta = 0.0142 \frac{\text{mmol/L}}{\Delta S_aO_2}$, $P = 0.003$) but remained unchanged ($P = 0.36$) after exposure to CO (Fig. 4D). The increase in lactate from exposure to hypoxic air was significantly different from the increase by CO exposure (poikilocapnic hypoxia: $P = 10^{-3}$, isocapnic hypoxia: $P = 0.017$). There was no significant difference between the increases in lactate between the poikilocapnic and isocapnic hypoxia groups ($P = 0.95$).

Measures of NAA and Cr + PCr were unaffected in all groups (Fig. 4E and F).

For the subgroup of subjects with S_aO_2 above 70% during the inhalation of hypoxic air ($n = 21$), SaO_2 averaged $79.1 \pm 5.0\%$, which is very similar to the saturations of the isocapnic hypoxia ($82.5 \pm 3.6\%$) and CO ($79.4 \pm 1.9\%$) groups. In the subgroup, we still observed a highly significant ($P < 10^{-4}$) increase in lactate of $0.0108 \frac{\text{mmol/L}}{\Delta S_aO_2}$ and a significant difference compared with exposure to CO ($P = 0.010$). We also still observed significantly higher CBF ($P < 10^{-6}$) and CDO_2 ($P < 10^{-6}$) responses in the CO group than in this subgroup.

Discussion

The major outcome of the present study was the finding of a robust increase in lactate concentration in the brain induced by inhalation of hypoxic air that was independent of changes in the rate of oxidative metabolism. Lactate production was observed both in the poikilocapnic and isocapnic hypoxia group, indicating a mechanism not related to hypocapnia. An upregulation of glycolysis with lactate as the end-product is therefore likely to be the effect of a mechanism that senses hypoxia and mediates the upregulation of glycolysis. This upregulation would then constitute a mechanism that protects against looming severe cerebral hypoxia. The released lactate would further work as a signaling molecule, potentially acting as an agent of vasodilatation, as discussed in the following.

The cause of this increase in lactate concentration is not readily apparent. Reduced oxygen metabolism will lead to a build-up of pyruvate in equilibrium with lactate as an end-product of glycolysis. However, as the $CMRO_2$ was unaffected, reduced oxygen metabolism is unlikely to be the cause of the elevated production. The group exposed to poikilocapnic hypoxic air had a small net decrease in CDO_2 (−10.5%). A decrease in CDO_2 of this magnitude is common and does not reduce cerebral oxygen consumption, for example, a cup of coffee causes caffeine-induced cerebral vasoconstriction and a decline in CDO_2 by 25–30% (Cameron et al. 1990; Gjedde et al. 2005).

Systemic lactate production and delivery to the brain cannot explain our findings, as previous studies have definitively demonstrated that acute short-term exposure to hypoxia does not significantly increase the systemic blood lactate when subjects remain inactive in an MRI scanner (Vestergaard et al. 2016; Jensen et al. 2018). Another potential cause of elevated lactate production could be the higher intracellular pH resulting from hyperventilation-induced tissue alkalosis. High pH levels stimulate the key glycolytic enzyme phosphofructokinase (PFK), resulting in upregulation of lactate production (Trivedi and Danforth 1966). Prior studies have also demonstrated increase in cerebral lactate concentration in response to hyperventilation but without hypoxia (Posse et al. 1997; Grüne et al. 2014). This possibility was tested by including a group exposed to isocapnic hypoxia by adding CO_2 to the inhaled hypoxic air to counteract hyperventilation-induced tissue alkalosis. In this isocapnic hypoxia group, we still observed a robust lactate production, demonstrating that a main mechanism involving increasing pH as the cause of lactate production is unlikely. Nevertheless, during poikilocapnic hypoxia, we would still expect an additive effect from hypocapnia causing further lactate production. However, we did not observe significant difference in the lactate production between the poikilocapnic and isocapnic hypoxia group, demonstrating that the additive effect from hypocapnia is minor compared with the hypoxia-induced production.

As lactate was produced without concomitant reduced oxygen metabolism and as we can preclude a main mechanism from alkalosis, the data suggest a mediated and fast upregulation of glycolysis as the cause for the lactate production. As exposure to CO did not result in an increase in lactate, a mechanism related to the difference in these two forms of insufficient oxygen delivery to the brain could be responsible for lactate production. The two main differences are that exposure to CO leads to a higher CBF response than inhalation of hypoxic air and that P_aO_2 is normal after CO exposure but reduced with hypoxic air. The oxygen pressure in the tissue can be moderately

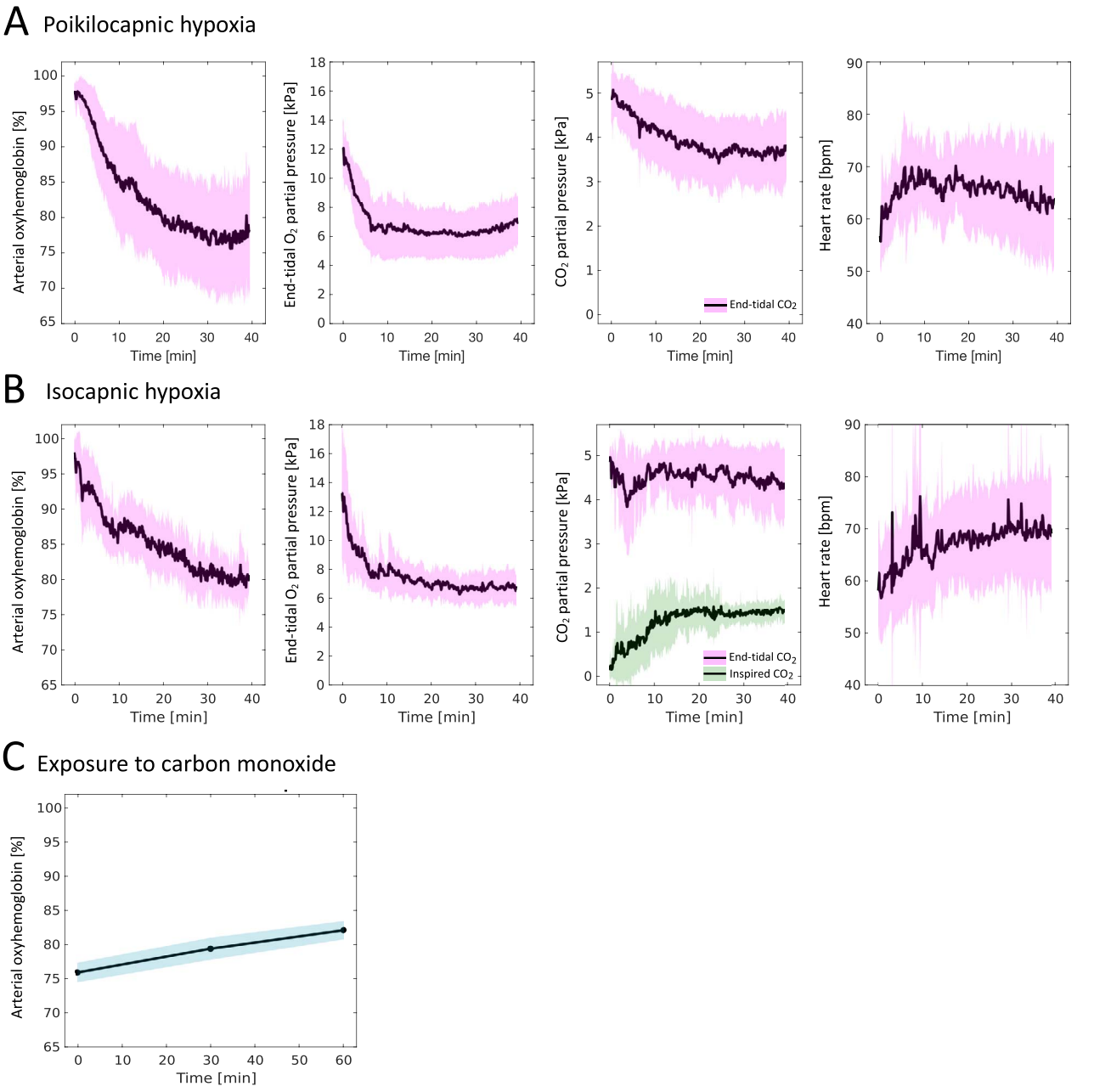

Figure 3. Arterial oxyhemoglobin saturation (S_aO_2), oxygen ($P_{et}O_2$), and CO_2 ($P_{et}CO_2$) end-tidal partial pressure and heart rate during poikilocapnic hypoxia (*A*) and isocapnic hypoxia (*B*). Oxyhemoglobin saturation after carbon monoxide exposure (*C*). Inhalation of hypoxic air was initiated at time point zero. Sequences for measuring CBF and $CMRO_2$ were acquired in the interval spanning 20–30 min after the start of the inhalation of hypoxic air or after CO exposure, and MRS measurements for lactate acquisition were recorded in the interval spanning ~30–40 min after start of exposures.

reduced in the cytosol of brain cells without affecting the $CMRO_2$ (Gjedde et al. 2005).

The main adaptive mechanism of cells to protect against hypoxia is regulated by HIF in the brain (Semenza and Wang 1992; Weidemann and Johnson 2008; Prabhakar and Semenza 2015). HIF accumulates in the cell when the intracellular oxygen pressure is reduced, and in response, HIF upregulates the expression of numerous genes related to metabolic adaptation to hypoxia, including increased angiogenesis, glucose transporters, erythropoietin expression, and glycolytic enzymes (Huang et al. 2012; Luo et al. 2012; Mergenthaler et al. 2012). The effects of higher gene expression are observed after several hours or days of hypoxic exposure. Whether a faster HIF-mediated pathway for upregulation of glycolysis within minutes exists, corresponding to the short-term hypoxic exposure seen in our study, is not known. Instead, the upregulation of glycolysis and lactate production could be mediated by reduced P_aO_2, as observed during inhalation of hypoxic air but not after CO exposure. Decreased P_aO_2 pressure is sensed at oxygen-chemosensitive sites of cells throughout the brain and mediates sympathetic stimulation (Gonzalez et al. 1994; Acker and Acker 2004; Neubauer and Sunderram 2004; López-Barneo et al. 2016; Marina et al. 2018).

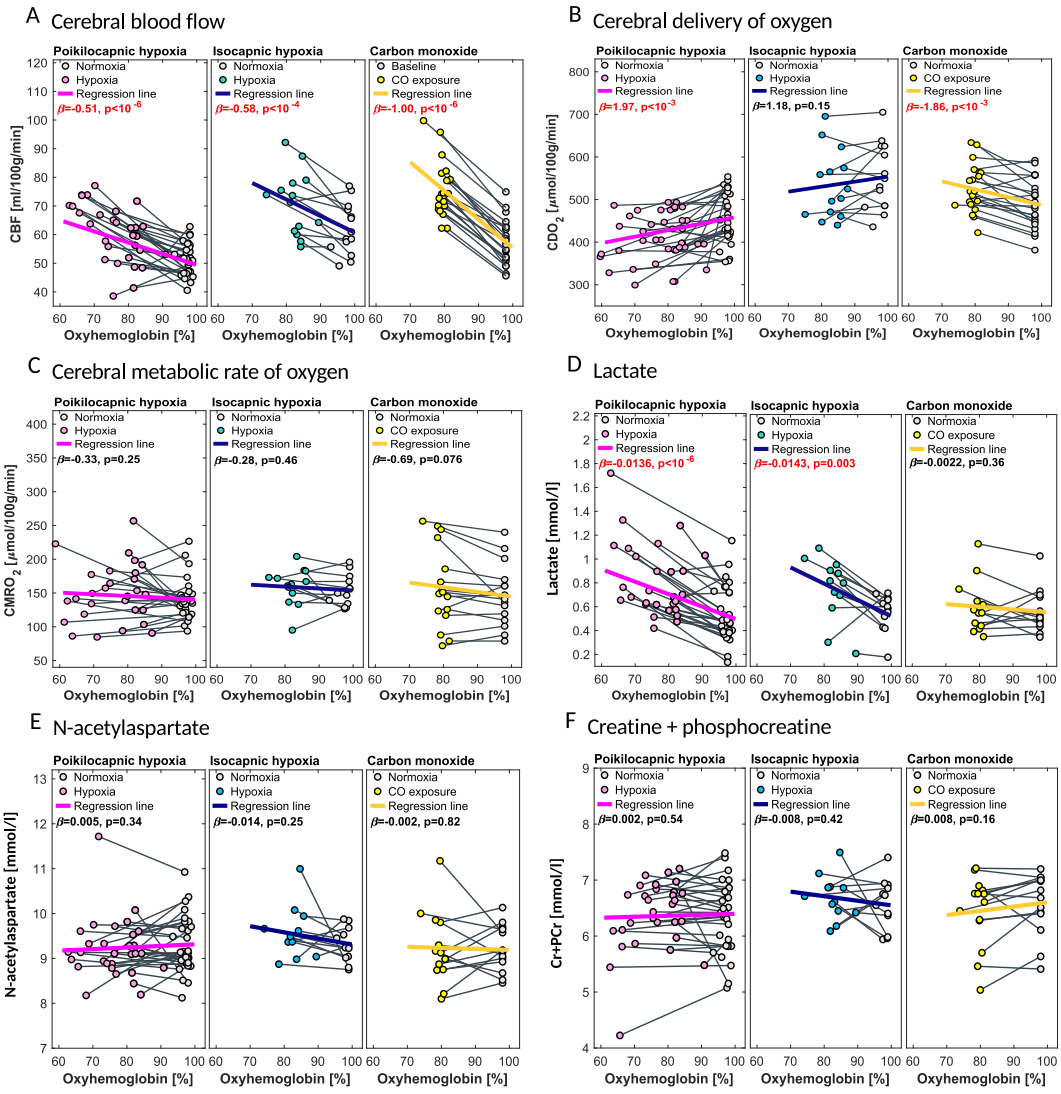

G

Group differences

	Poikilocapnic hypo. vs. isocap. hypo. p-values	Poikilocapnic hypo. vs. CO p-value	Isocap. hypo. vs. CO p-values
CBF	0.61	$<10^{-6}$	$<10^{-3}$
CDO_2	0.52	$<10^{-5}$	$<10^{-3}$
$CMRO_2$	0.93	0.47	0.47
Lactate	0.95	$<10^{-3}$	0.017
NAA	0.11	0.51	0.43
Cr+PCr	0.36	0.45	0.21

Figure 4. (*A*) Change in cerebral blood flow (CBF), (*B*) cerebral delivery of oxygen (CDO_2), (*C*) cerebral metabolic rate of oxygen ($CMRO_2$), (*D*) cerebral lactate concentration, (*E*) N-acetylaspartate (NAA) concentration, and (*F*) creatine + phosphocreatine (Cr + PCr) concentration after exposure to poikilocapnic hypoxia, isocapnic hypoxia, or carbon monoxide. The panels present correlations between desaturation and the cerebral physiology measures with the results from the linear mixed models. The regression coefficients (β) and *P*-values from the regressions are noted in each panel. The results of the model testing whether the regression coefficients were significantly different among the three groups are presented in the table (*G*). CBF increased in all groups but with a significantly higher response to CO exposure (poikilocapnic hypoxia: $P < 10^{-6}$, isocapnic hypoxia: $P < 10^{-3}$). CDO_2 decreased in the poikilocapnic hypoxia group ($P < 10^{-3}$), was unchanged after isocapnic hypoxia ($P = 0.15$), and increased after CO exposure ($P < 10^{-3}$). The lactate concentration increased in the two groups inhaling hypoxic air (poikilocapnic hypoxia: $P < 10^{-4}$, isocapnic hypoxia: $P = 0.003$) but not from CO exposure ($P = 0.36$). The $CMRO_2$, NAA concentration, and Cr + PCr concentration were unchanged in all groups.

Sympathetic stimulation of the central nervous system initiates multiple compensatory mechanisms, including increased ventilation and heart rate, but also affects cells by increasing brain glucose uptake and oxygen usage (Whipp and Wasserman 1980; Dienel and Cruz 2016; Joyner et al. 2018). Similar activation may not be seen from CO exposure; for example, carotid or aortic chemoreceptors are not engaged by moderate CO stimulation (Duke et al. 1952; Lahiri et al. 1981). In addition, exposure to CO resulted in a net increase in cerebral oxygen delivery (7.8%), which would ensure normal oxygen pressure in the cells, which may explain the missing chemoreceptor stimulation from hypoxia in the CO group.

Hypoxic upregulation of glycolysis with lactate production could constitute a protective mechanism by rapidly providing adenosine triphosphate (ATP) and nicotinamide adenine dinucleotide (NADH) - type to be utilized if the hypoxia becomes more severe. In addition, the resulting lactate could serve as a signaling molecule. The hypothesis of lactate as a signaling molecule and as a regulator of multiple metabolic pathways in the brain has recently gained traction (Bergersen and Gjedde 2012; Bergersen 2015; Mosienko et al. 2015; Magistretti and Allaman 2018). It was recently discovered that lactate-activated hydroxycarboxylic acid receptor 1 (HCAR1) (also called the G-protein-coupled lactate receptor GPR81) is present throughout the brain, including in neurons, glial cells, and cerebral blood vessels (Lauritzen et al. 2014). In addition, monocarboxylate transporters are widely distributed in the brain, enabling the transport of lactate along its concentration gradients from sites of production to neighboring cells.

The signaling roles of lactate in the brain remain to be fully described, and multiple pathways may exist. A possible role for lactate is regulation of cell redox and NADH to NAD+ balances when pyruvate is converted to lactate by lactate dehydrogenase (Yang et al. 2014; Jourdain et al. 2016), as also observed in skeletal muscle cells (Brooks 2009). An increase in NADH by the conversion of lactate to pyruvate potentiates N-methyl-D-aspartate (NMDA)-type glutamate receptor activity, which has downstream cascade effects, promoting the expression of plasticity genes (Yang et al. 2014). Lactate may also protect against excitotoxicity, where lactate transported into neurons opens K^+-ATP channels through activation of the phosphatidylinositol 3′-kinase cascade pathways that lead to hyperpolarization of the cell (Jourdain et al. 2016). In experimental cell studies, lactate has been found to regulate the excitability and activation of neurons by a receptor-mediated mechanism in both excitatory (Tang et al. 2014) and inhibitory directions (Bozzo et al. 2013). Lactate also appears to have a long-term regulatory effect by activating the expression of the brain-derived neurotropic factor and N-muc downstream regulated gene3 (NDRG3) proteins that stimulate pathways to increase angiogenesis, neurogenesis, and cell growth (Lee et al. 2015; El Hayek et al. 2019). In addition, activation of HCAR1 attenuates cyclic adenosinemonophosphate (cAMP) levels, where reduced cAMP inhibits glycolysis and provides negative feedback for the regulation of lactate production (Lauritzen et al. 2014), as is commonly seen for regulatory molecules.

In the present study, the most important short-term signaling role of lactate could be as a vasodilating agent. Lactate is an important mediator of vasodilation, which is part of the neurovascular coupling during neuronal activation (Gordon et al. 2008; Attwell et al. 2010). Neuronal activation initiates rapid lactate formation from both neurons and astrocytes. The released lactate regulates the prostaglandin vasomotor effect of the arterioles, promoting vasodilation (Mintun et al. 2004; Gordon et al. 2008). Cell studies on retinal samples have similarly demonstrated vasodilation from extracellular lactate (Hein et al. 2006; Yamanishi et al. 2006). In these studies, the pH levels were maintained when lactate was added, demonstrating a vasodilation effect independent of pH changes.

If lactate production, and the consequent regulation of vasodilation, is a part of the protective cerebrovascular response to hypoxia, then a reduced capability for lactate production could be harmful to the brain. We previously demonstrated that patients with obstructive sleep apnea (OSA) have both reduced CBF and lactate responses to hypoxic exposure (Jensen et al. 2018). Reduced protection by lactate could be the cause of the attenuated CBF response seen in these patients. Patients with OSA have a severely increased risk of stroke and future neurodegenerative disease, compatible with reduced cerebrovascular function. Whether reduced lactate production from moderate hypoxic stimuli also correlates with reduced CVR function in neurodegenerative disease or other brain diseases remains to be examined.

We observed the largest CBF response in the CO group, showing that lactate is not invariably involved in the facilitation of vasodilation. Rather, the large CBF increase seen in this group could be cerebral vasodilation promoted by CO by a separate pathway, independent of the pathway activated after exposure to hypoxic air. We consider such a mechanism to be more significant than the centerwards shift of the oxyhemoglobin dissociation curve seen after CO exposure (Paulson 1973). Thus, it appears that CO has a direct vasodilatory effect on vascular smooth muscle cells, independent of tissue hypoxia or metabolism (Furchgott and Jothianandan 1991; Wang et al. 1997). CO-induced vasodilation could work by activating calcium-gated potassium channels (K_{Ca} channels) or the cyclic guanosine monophosphate (GMP) pathway in smooth muscle cells, similar to the effect of nitrogen oxide (NO) (Wang et al. 1997).

The combined Cr + PCr concentrations were unaffected in all groups. Cr + PCr in the brain can work as energy reserves with ATP rapidly produced from creatine kinase. Animal models have shown that ATP reduction from severe hypoxia is associated with reduced phosphocreatine concentrations (Tsuji et al. 1995). The unaffected combined Cr + PCr concentrations further demonstrated that energy metabolism and ATP availability were not reduced by the moderately hypoxic stimuli used in the present study, equivalent to the maintained $CMRO_2$.

Strengths and Limitations

To the best of our knowledge, the present study is the first to directly compare cerebral lactate production in response to multiple hypoxic stimuli in humans. By acquiring cerebral lactate concentrations, we recorded a compound that is both a biomarker of glycolysis and a potential signaling molecule related to vasodilation. By acquiring near-simultaneous metrics for CBF and $CMRO_2$, we obtained the necessary results that allowed us to hypothesize about the origin of lactate production, which was not evident from prior studies.

A drawback of this study is the unpaired experimental setup with three separate groups. By using a paired setup, the statistical power of the experiment would increase. However, as we observed highly statistically significant results using

appropriate unpaired statistics, the study was not underpowered, and a paired setup would be expected to yield similar results. We therefore do not consider the unpaired setup to be a major limitation.

Global CBF acquired by PCM has been validated in pigs and animals against ^{15}O-water positron emmision tomography (PET) imaging as the accepted gold standard reference (Vestergaard et al. 2017; Ssali et al. 2018; Puig et al. 2019). Measurements of oxygen saturation in the sagittal sinus for $CMRO_2$ calculation by the SBO MRI technique have been validated against blood samples acquired by catheter from the jugular vein during MRI scanning (Miao et al. 2019). Validation was performed both at rest and during hypoxic and hypercapnic conditions (Miao et al. 2019).

Absolute quantification of brain metabolites using MRS has potentially confounding factors related to the scanner sequence, magnetic field homogeneity, and function of the MRI scanner (Jansen et al. 2006). Hypoxemia of brain circulation will change the magnetic properties of the arterial blood and potentially could affect the magnetic field in the scanner, confounding the acquired spectra and biasing the hypoxia measurement. However, the unaffected NAA concentrations suggest that there were no systematic errors caused by changes in the magnetic field, as NAA would not physiologically be affected by short periods of exposure to hypoxia, although it is sensitive to the effects of confounding changes in the magnetic field. In addition, as we performed a paired comparison of the same subject in two situations, the problems of absolute concentrations were mitigated.

We note that carboxyhemoglobin has magnetic properties similar to those of oxyhemoglobin (Pauling and Coryell 1936), and CO exposure therefore has no unknown effects on the acquired MRI signals.

Oxygen and CO_2 blood gas pressures were not acquired by arterial blood sampling, and instead, we used end-tidal measurements as surrogates in the group inhaling hypoxic air. End-tidal O_2 and CO_2 pressures were not acquired in the CO group, but prior studies, with identical delivery of CO, have demonstrated that $P_{et}O_2$, $P_{et}CO_2$, and respiration frequency were unaffected by moderate CO exposure (Arngrim et al. 2018; Ghanizada et al. 2018).

In conclusion, we demonstrated that lactate production in response to moderate hypoxia in healthy humans is not the result of impaired oxidative metabolism or hyperventilation-induced alkalosis. Instead, a more likely main cause of lactate production is the upregulation of glycolysis due to the effects of hypoxia. Upregulation of glycolysis with lactate as the end-product could constitute a protective mechanism initiated before the advent of cell-threatening hypoxia. The released lactate works as a signaling molecule, perhaps regulating vasodilatation.

Authors' Contribution

M.B.V. and H.B.W.L. conceived the experiment. M.B.V., H.B.W.L., N.A., O.B.P., and M.A. contributed to the design and implementation of the research. H.G., N.A., M.B.V., and H.B.W.L. collected the data. M.B.V., H.G., and U.L. analyzed and calculated the data. A.G. contributed to the interpretation of the observed lactate production. All authors participated in the interpretation of the results. The manuscript was prepared by M.B.V. and critically revised by the remaining authors. All authors approved the final manuscript.

Funding

The Danish Council for Independent Research (8020-00251B); Rigshospitalets Forskningspulje and Lundbeck Foundation (R155-2014-171).

Notes

Conflict of Interest: M.A. is a consultant, speaker, or scientific advisor for AbbVie, Allergan, Amgen, Alder, Biohaven, Eli Lilly, Lundbeck, Novartis, and Teva and a primary investigator for Alder, Amgen, Allergan, Eli Lilly, Lundbeck, Novartis, and Teva trials. M.A. has no ownership interest and does not own stocks of any pharmaceutical company. M.A. serves as associate editor of Cephalalgia and associate editor of the Journal of Headache and Pain. M.A. is president of the International Headache Society.

References

Acker T, Acker H. 2004. Cellular oxygen sensing need in CNS function: physiological and pathological implications. *J Exp Biol*. 207:3171–3188.

Arngrim N, Schytz HW, Britze J, Vestergaard MB, Sander M, Olsen KS, Olesen J, Ashina M. 2018. Carbon monoxide inhalation induces headache in a human headache model. *Cephalalgia*. 38:697–706.

Attwell D, Buchan AM, Charpak S, Lauritzen M, Macvicar B, Newman E. 2010. Glial and neuronal control of brain blood flow. *Nature*. 468:232–243.

Bakker CJG, Hartkamp MJ, Mali WPTM. 1996. Measuring blood flow by nontriggered 2D phase-contrast MR angiography. *Magn Reson Imaging*. 14:609–614.

Bergersen LH. 2015. Lactate transport and signaling in the brain: potential therapeutic targets and roles in body-brain interaction. *J Cereb Blood Flow Metab*. 35:176–185.

Bergersen LH, Gjedde A. 2012. Is lactate a volume transmitter of metabolic states of the brain? *Front Neuroenergetics*. 4:1–6.

Bozzo L, Puyal J, Chatton JY. 2013. Lactate modulates the activity of primary cortical neurons through a receptor-mediated pathway. *PLoS One*. 8:1–9.

Brooks GA. 2009. Cell-cell and intracellular lactate shuttles. *J Physiol*. 587:5591–5600.

Cameron O, Modell J, Hariharan M. 1990. Caffeine and human cerebral blood flow: a positron emission tomography study. *Life Sci*. 47:1141–1146.

Christiansen P, Henriksen O, Stubgaard M, Gideon P, Larsson HBW. 1993. In vivo quantification of brain metabolites by 1H-MRS using water as an internal standard. *Magn Reson Imaging*. 11:107–118.

Dienel GA, Cruz NF. 2016. Aerobic glycolysis during brain activation: adrenergic regulation and influence of norepinephrine on astrocytic metabolism. *J Neurochem*. 138:14–52.

Duke HN, Green JH, Neil E. 1952. Carotid chemoceptor impulse activity during inhalation of carbon monoxide mixtures. *J Physiol*. 118:520–527.

El Hayek L, Khalifeh M, Zibara V, Abi Assaad R, Emmanuel N, Karnib N, El-Ghandour R, Nasrallah P, Bilen M, Ibrahim P, et al. 2019. Lactate mediates the effects of exercise on learning and memory through sirt1-dependent activation of hippocampal brain-derived neurotrophic factor (BDNF). *J Neurosci*. 39:2369–2382.

Furchgott RF, Jothianandan D. 1991. Endothelium-dependent and -independent vasodilation involving cyclic GMP: relaxation induced by nitric oxide, carbon monoxide and light. *Blood Vessels*. 28:52–61.

Ghanizada H, Arngrim N, Schytz HW, Olesen J, Ashina M. 2018. Carbon monoxide inhalation induces headache but no migraine in patients with migraine without aura. *Cephalalgia*. 38:1940–1949.

Gjedde A, Johannsen P, Cold GE, Østergaard L. 2005. Cerebral metabolic response to low blood flow: possible role of cytochrome oxidase inhibition. *J Cereb Blood Flow Metab*. 25:1183–1196.

Gonzalez C, Almaraz L, Obeso A, Rigual R. 1994. Carotid body chemoreceptors: from natural stimuli to sensory discharges. *Physiol Rev*. 74:829–898.

Gordon GRJ, Choi HB, Rungta RL, Ellis-Davies GCR, MacVicar BA. 2008. Brain metabolism dictates the polarity of astrocyte control over arterioles. *Nature*. 456:745–749.

Greijer AE, Van Der Wall E. 2004. The role of hypoxia inducible factor 1 (HIF-1) in hypoxia induced apoptosis. *J Clin Pathol*. 57:1009–1014.

Grüne F, Kazmaier S, Sonntag H, Stolker RJ, Weyland A. 2014. Moderate hyperventilation during intravenous anesthesia increases net cerebral lactate efflux. *Anesthesiology*. 120:335–342.

Gujarati D. 1970. Use of dummy variables in testing for equality between sets of coefficients in linear regressions. *Am Stat*. 24:18–22.

Harris AD, Roberton VH, Huckle DL, Saxena N, Evans CJ, Murphy K, Hall JE, Bailey DM, Mitsis G, Edden R, et al. 2013. Temporal dynamics of lactate concentration in the human brain during acute inspiratory hypoxia. *J Magn Reson Imaging*. 37:739–745.

Hein TW, Xu W, Kuo L. 2006. Dilation of retinal arterioles in response to lactate: role of nitric oxide, guanylyl cyclase, and ATP-sensitive potassium channels. *Invest Ophthalmol Vis Sci*. 47:693–699.

Huang Y, Lei L, Liu DG, Jovin I, Russell R, Johnson RS, Di Lorenzo A, Giordano FJ. 2012. Normal glucose uptake in the brain and heart requires an endothelial cell-specific HIF-1α-dependent function. *Proc Natl Acad Sci U S A*. 109:17478–17483.

Jain V, Langham MC, Floyd TF, Jain G, Magland JF, Wehrli FW. 2011. Rapid magnetic resonance measurement of global cerebral metabolic rate of oxygen consumption in humans during rest and hypercapnia. *J Cereb Blood Flow Metab*. 31:1504–1512.

Jain V, Langham MC, Wehrli FW. 2010. MRI estimation of global brain oxygen consumption rate. *J Cereb Blood Flow Metab*. 30:1598–1607.

Jansen JFA, Backes WH, Nicolay K, Kooi ME. 2006. 1H MR spectroscopy of the brain: absolute quantification of metabolites. *Radiology*. 240:318–332.

Jenkinson M, Beckmann CF, Behrens TEJ, Woolrich MW, Smith SM. 2012. Fsl. *Neuroimage*. 62:782–790.

Jensen MLF, Vestergaard MB, Tønnesen P, Larsson HBW, Jennum PJ. 2018. Cerebral blood flow, oxygen metabolism, and lactate during hypoxia in patients with obstructive sleep apnea. *Sleep*. 41:1–10.

Jourdain P, Allaman I, Rothenfusser K, Fiumelli H, Marquet P, Magistretti PJ. 2016. L-lactate protects neurons against excitotoxicity: implication of an ATP-mediated signaling cascade. *Sci Rep*. 6:21250.

Joyner MJ, Limberg JK, Wehrwein EA, Johnson BD. 2018. Role of the carotid body chemoreceptors in glucose homeostasis and thermoregulation in humans. *J Physiol*. 596:3079–3085.

Lahiri S, Mulligan E, Nishino T, Mokashi A, Davies RO. 1981. Relative responses of aortic body and carotid body chemoreceptors to carboxyhemoglobinemia. *J Appl Physiol*. 50:580–586.

Lauritzen KH, Morland C, Puchades M, Holm-Hansen S, Hagelin EM, Lauritzen F, Attramadal H, Storm-Mathisen J, Gjedde A, Bergersen LH. 2014. Lactate receptor sites link neurotransmission, neurovascular coupling, and brain energy metabolism. *Cereb Cortex*. 24:2784–2795.

Lee DC, Sohn HA, Park KC, Yeom YI, Lee DC, Sohn HA, Park Z, Oh S, Kang YK, Lee K, et al. 2015. A lactate-induced response to hypoxia. *Cell*. 161:595–609.

Li C, Langham MC, Epstein CL, Magland JF, Wu J, Gee J, Wehrli FW. 2012. Accuracy of the cylinder approximation for susceptometric measurement of intravascular oxygen saturation. *Magn Reson Med*. 67:808–813.

López-Barneo J, Ortega-Sáenz P, González-Rodríguez P, Fernández-Agüera MC, Macías D, Pardal R, Gao L. 2016. Oxygen-sensing by arterial chemoreceptors: mechanisms and medical translation. *Mol Aspects Med*. 47–48:90–108.

Luo J, Martinez J, Yin X, Sanchez A, Tripathy D, Grammas P. 2012. Hypoxia induces angiogenic factors in brain microvascular endothelial cells. *Microvasc Res*. 83:138–145.

Magistretti PJ, Allaman I. 2018. Lactate in the brain: from metabolic end-product to signalling molecule. *Nat Rev Neurosci*. 19:235–249.

Marina N, Turovsky E, Christie IN, Hosford PS, Hadjihambi A, Korsak A, Ang R, Mastitskaya S, Sheikhbahaei S, Theparambil SM, et al. 2018. Brain metabolic sensing and metabolic signaling at the level of an astrocyte. *Glia*. 66: 1185–1199.

Mergenthaler P, Kahl A, Kamitz A, Van Laake V, Stohlmann K, Thomsen S, Klawitter H, Przesdzing I, Neeb L, Freyer D, et al. 2012. Mitochondrial hexokinase II (HKII) and phosphoprotein enriched in astrocytes (PEA15) form a molecular switch governing cellular fate depending on the metabolic state. *Proc Natl Acad Sci U S A*. 109:1518–1523.

Miao X, Nayak KS, Wood JC. 2019. In vivo validation of T2- and susceptibility-based SvO2 measurements with jugular vein catheterization under hypoxia and hypercapnia. *Magn Reson Med*. 82:2188–2198.

Mintun MA, Vlassenko AG, Rundle MM, Raichle ME. 2004. Increased lactate/pyruvate ratio augments blood flow in physiologically activated human brain. *Proc Natl Acad Sci U S A*. 101:659–664.

Mosienko V, Teschemacher AG, Kasparov S. 2015. Is L-lactate a novel signaling molecule in the brain? *J Cereb Blood Flow Metab*. 35:1069–1075.

Neubauer JA, Sunderram J. 2004. Oxygen-sensing neurons in the central nervous system. *J Appl Physiol*. 96:367–374.

Overgaard M, Rasmussen P, Bohm AM, Seifert T, Brassard P, Zaar M, Homann P, Evans KA, Nielsen HB, Secher NH. 2012. Hypoxia and exercise provoke both lactate release and lactate oxidation by the human brain. *FASEB J*. 26:3012–3020.

Pauling L, Coryell CD. 1936. The magnetic properties and structure of hemoglobin, oxyhemoglobin and carbonmonoxyhemoglobin. *Proc Natl Acad Sci*. 22:210–216.

Paulson OB, Parving HH, Olesen J, Skinhoj E. 1973. Influence of carbon monoxide and of hemodilution on cerebral blood flow and blood gases in man. *J Appl Physiol*. 35: 111–116.

Posse S, Dager SR, Richards TL, Yuan C, Ogg R, Artru AA, Müller-Gärtner HW, Hayes C. 1997. In vivo measurement of regional brain metabolic response to hyperventilation using magnetic

resonance: proton echo planar spectroscopic imaging (PEPSI). *Magn Reson Med*. 37:858–865.

Prabhakar NR, Semenza GL. 2015. Oxygen sensing and homeostasis. *Physiology*. 30:340–348.

Puig O, Vestergaard MB, Lindberg U, Hansen AE, Ulrich A, Andersen FL, Johannesen HH, Rostrup E, Law I, Larsson HBW, et al. 2019. Phase contrast mapping MRI measurements of global cerebral blood flow across different perfusion states – a direct comparison with 15O-H2O positron emission tomography using a hybrid PET/MR system. *J Cereb Blood Flow Metab*. 39:2368–2378.

Quadrelli S, Mountford C, Ramadan S. 2016. Hitchhiker's guide to voxel segmentation for partial volume correction of in vivo magnetic resonance spectroscopy. *Magn Reson Insights*. 9:1–8.

Rodgers ZB, Leinwand SE, Keenan BT, Kini LG, Schwab RJ, Wehrli FW. 2016. Cerebral metabolic rate of oxygen in obstructive sleep apnea at rest and in response to breath-hold challenge. *J Cereb Blood Flow Metab*. 36:755–767.

Semenza GL. 2012. Hypoxia-inducible factors in physiology and medicine. *Cell*. 148:399–408.

Semenza GL, Wang GL. 1992. A nuclear factor induced by hypoxia via de novo protein synthesis binds to the human erythropoietin gene enhancer at a site required for transcriptional activation. *Mol Cell Biol*. 12:5447–5454.

Sendoel A, Hengartner MO. 2014. Apoptotic cell death under hypoxia. *Physiology*. 29:168–176.

Ssali T, Anazodo UC, Thiessen JD, Prato FS, St Lawrence K. 2018. A noninvasive method for quantifying cerebral blood flow by hybrid PET/MRI. *J Nucl Med*. 59:1329–1334.

Tang F, Lane S, Korsak A, Paton JFR, Gourine AV, Kasparov S, Teschemacher AG. 2014. Lactate-mediated glia-neuronal signalling in the mammalian brain. *Nat Commun*. 5:1–13.

Torack RM, Alcala H, Gado M, Burton R. 1976. Correlative assay of computerized cranial tomography (CCT), water content and specific gravity in normal and pathological postmortem brain. *J Neuropathol Exp Neurol*. 35:385–392.

Trivedi B, Danforth WH. 1966. Effect of pH on the kinetics of frog muscle phosphofructokinase. *J Biol Chem*. 241:4110–4114.

Tsuji M, Allred E, Jensen F, Holtzman D. 1995. Phosphocreatine and ATP regulation in the hypoxic developing rat brain. *Brain Res Dev Brain Res*. 85:192–200.

Vafaee MS, Vang K, Bergersen LH, Gjedde A. 2012. Oxygen consumption and blood flow coupling in human motor cortex during intense finger tapping: implication for a role of lactate. *J Cereb Blood Flow Metab*. 32:1859–1868.

Vestergaard MB, Jensen MLF, Arngrim N, Lindberg U, Larsson HBW. 2020. Higher physiological vulnerability to hypoxic exposure with advancing age in the human brain. *J Cereb Blood Flow Metab*. 40:341–353.

Vestergaard MB, Larsson HBW. 2019. Cerebral metabolism and vascular reactivity during breath-hold and hypoxic challenge in freedivers and healthy controls. *J Cereb Blood Flow Metab*. 39:834–848.

Vestergaard MB, Lindberg U, Aachmann-Andersen NJ, Lisbjerg K, Christensen SJ, Law I, Rasmussen P, Olsen NV, Larsson HBW. 2016. Acute hypoxia increases the cerebral metabolic rate – a magnetic resonance imaging study. *J Cereb Blood Flow Metab*. 36:1046–1058.

Vestergaard MB, Lindberg U, Aachmann-Andersen NJ, Lisbjerg K, Christensen SJ, Rasmussen P, Olsen NV, Law I, Larsson HBW, Henriksen OM. 2017. Comparison of global cerebral blood flow measured by phase-contrast mapping MRI with 15O-H2O positron emission tomography. *J Magn Reson Imaging*. 45:692–699.

Wang R, Wang Z, Wu L. 1997. Carbon monoxide-induced vasorelaxation and the underlying mechanisms. *Br J Pharmacol*. 121:927–934.

Weidemann A, Johnson RS. 2008. Biology of HIF-1α. *Cell Death Differ*. 15:621–627.

Whipp BJ, Wasserman K. 1980. Carotid bodies and ventilatory control dynamics in man. *Fed Proc*. 39:2668–2673.

Xu W, Chi L, Row BW, Xu R, Ke Y, Xu B, Luo C, Kheirandish L, Gozal D, Liu R. 2004. Increased oxidative stress is associated with chronic intermittent hypoxia-mediated brain cortical neuronal cell apoptosis in a mouse model of sleep apnea. *Neuroscience*. 126:313–323.

Yamanishi S, Katsumura K, Kobayashi T, Puro DG. 2006. Extracellular lactate as a dynamic vasoactive signal in the rat retinal microvasculature. *Am J Physiol Heart Circ Physiol*. 290:925–934.

Yang J, Ruchti E, Petit JM, Jourdain P, Grenningloh G, Allaman I, Magistretti PJ. 2014. Lactate promotes plasticity gene expression by potentiating NMDA signaling in neurons. *Proc Natl Acad Sci U S A*. 111:12228–12233.

Zhang X, Le W. 2010. Pathological role of hypoxia in Alzheimer's disease. *Exp Neurol*. 223:299–303.